Permeability and Strength of Core Samples from the Nojima Fault of the 1995 Kobe Earthquake

David Lockner[1], Hisanobu Naka[2], Hidemi Tanaka[2], Hisao Ito[3], and Ryuji Ikeda[4]

[1] *US Geological Survey, 345 Middlefield Rd MS977, Menlo Park, CA 94025, USA; dlockner@isdmnl.wr.usgs.gov*
[2] *Ehime University, Matsuyama, Japan*
[3] *Geological Survey of Japan, Tsukuba, Japan*
[4] *National Research Institute for Earth Science and Disaster Prevention, Tsukuba, Japan*

ABSTRACT

The 1995 Hyogoken-Nanbu (Kobe) earthquake, M=7.2, ruptured the Nojima fault. We have studied core samples taken from two scientific drillholes which crossed the fault zone in the epicentral region on Awagi island. The shallower hole, drilled by the Geological Survey of Japan (GSJ), was started 75m to the SE of the surface trace of the Nojima fault and crossed the fault at a depth of 624m. A deeper hole, drilled by the National Research Institute for Earth Science and Disaster Prevention (NIED) was started 302m to the SE of the fault and crossed fault strands below a depth of 1140m. We have measured strength and matrix permeability of core samples taken from these two drillholes. We find a strong correlation between permeability and proximity to the fault zone shear axes. The width of the high permeability zone (approximately 20 to 40m) is in good agreement with fault zone width inferred from trapped wave analysis and other evidence. The fault zone core or shear axis contains clays with permeabilities of approximately 0.1 to 1 microdarcy at 50 MPa confining pressure. Within a few meters of the fault zone core, the rock is highly fractured but has sustained little net shear. Matrix permeability of this zone is approximately 100 microdarcy at 50 MPa confining pressure. Outside this damage zone, matrix permeability drops to sub-nanodarcy values. The clay-rich core material has the lowest strength with a coefficient of friction of approximately 0.55. Shear strength gradually increases with distance from the shear axis. These permeability and strength observations are consistent with fault zone models in which a highly localized core or shear zone is surrounded by a damage zone of fractured rock. In this case, the damage zone will act as a high-permeability conduit for vertical and horizontal flow in the plane of the fault. The clay core region, however, will impede fluid flow across the fault.

INTRODUCTION

The scientific drillholes crossing the Nojima fault at depth in the epicentral region of the 1995 Kobe earthquake, M=7.2, provide a unique opportunity to study the mechanical and fluid transport properties of an active fault immediately after a major rupture event. Most first hand evidence of the properties of active faults comes from examination of surface exposures which have typically undergone long and complicated histories of uplift and alteration. Examination of fault rock associated with rupture nucleation or significant energy release on strike-slip faults presents a particular problem since there is little vertical slip to bring deeper rocks to the surface. Seismic, gravity, electromagnetic and other remote sensing techniques can provide information about the deep structure of active faults, but a complete understanding of fault zone properties in the hypocentral regions of damaging earthquakes will require direct observation by the drilling of deep scientific boreholes.

Numerous laboratory and field observations have shown that earthquakes, representing the dynamic faulting process in the brittle crust, involve breaking and crushing of grains and the progressive growth of the fault zone. A typical fault zone structure, as suggested by studies of exhumed faults [*Chester et al.*, 1993; *Caine et al.*, 1996; *Caine and Forster*, 1999], includes a narrow clay-rich or fine-grained core surrounded by a damage zone of highly fractured rock. The bulk of the shear deformation associated with the fault occurs in the narrow core zone, implying that this is the weakest portion of the fault structure. However, due to the fine grain size of the clay or crushed material in the fault core, it is expected to have a relatively low permeability.

The surrounding damage zone contains a high density of microcracks, both within and between grains, but is likely to have sustained relatively little total strain. Similar structures have been observed in laboratory samples that have been loaded to failure [*Moore and Lockner*, 1995]. If the fault occurs in low-porosity crystalline rock (such as the Nojima fault), the high crack density in the damage zone results in significant pore volume increase and an increase in transport properties such as fluid permeability [*Caine et al.*, 1996; *Caine and Forster*, 1999] and electrical conductivity [*Lockner and Byerlee*, 1986]. The contrast in material properties between damage zones associated with active faults and the surrounding country rock can often be observed with remote geophysical techniques such as magnetotelluric and seismic profiling. Most recently, trapped seismic waves, in which the fault zone acts as a waveguide, have been observed in active faults [*Li and Leary*, 1990; *Ben-Zion*, 1998], and in particular on the Nojima fault [*Li et al.*, 1998].

In the present study, we report on laboratory tests of 22 core samples taken from the NIED and GSJ drillholes following the Kobe earthquake. Rock strength and matrix permeability measurements were carried out to provide fault zone properties for profiles across the fault at two depths. Due to the limited number of samples and the difficulties associated with sample preparation, this study was intended to be exploratory in nature. In fact, the permeability and strength measurements are in excellent agreement with the idealized fault structural model described above. The GSJ borehole showed a single clay-rich shear zone at a depth of 624 m. The NIED hole showed two clay-rich shear zones at depths of 1140 m and 1320 m. A more diffuse shear zone was also crossed at about 1800 m (see Fig. 1). These three zones are referred to, respectively, in this paper as the shallow, intermediate and deep NIED shear zones. Strength and permeability measurements reported here, as well as petrographic observations presented by Moore (this volume), all indicate that unlike the other shear zone crossings, the deep shear zone was not activated by the 1995 Kobe earthquake.

EXPERIMENTAL TECHNIQUE

Protolith rock for the Nojima fault in the vicinity of the boreholes is a biotite-hornblende granodiorite (see, for example, Moore in this volume). A set of 22 samples were selected from the NIED and GSJ boreholes. Due to this limited number, sample selection was concentrated about the obvious shear zones in an attempt to obtain representative profiles across the fault zone structures. Significant variability of rock type exists in the shear zones and a more complete evaluation of fault zone properties would require a much denser and more systematic sampling of the core than was possible in this study. Preferred sample dimensions were nominally 25.4 mm-diameter by 50.8 mm-length cylinders. Much of the core (especially in the damage zones) had little or no cohesion and contained hard grain fragments. As a result, many samples were impossible to prepare to these preferred dimensions. Most samples that could not be prepared as cylinders were cut into rectangular prisms with 18.0 mm-square cross-sections. The clay-rich shear zone core samples were available in limited quantities and sliced to provide 2-mm-thick wafers. These were placed between porous sandstone driving blocks cut at an angle of 30° to the sample axis.

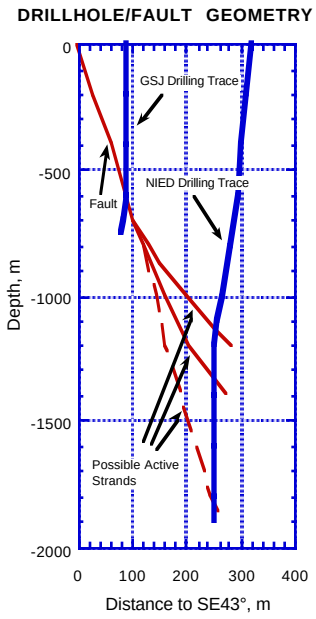

Figure 1. Schematic diagram of the Nojima fault in the vicinity of the JSG and NIED drillholes, showing the depths at which shear zones were intersected.

Samples were jacketed and loaded in a standard triaxial deformation apparatus. Each sample was evacuated and then saturated with

distilled, deionized water. Permeability was measured using a constant flow rate method at effective confining pressure of 10, 30, and 50 MPa. Test samples were oriented parallel to the original borehole cores so that the reported permeability and strength data are essentially for flow and maximum compressive stress oriented subvertically. No attempt was made to determine anisotropy in either permeability or strength. Following the hydrostatic permeability measurements, each sample was loaded incrementally at constant effective confining pressure of 50 MPa until failure occurred. Following each strain increment along the loading path, deformation was halted and permeability was determined as indicated in Fig. 2. After peak stress, deformation continued to 5 mm axial shortening at a rate of 1 µm/sec with periodic pauses to repeat permeability measurements.

Accuracy of the permeability measurements is difficult to determine since some samples had less than ideal surface finishes and some permeabilities were near both the high and low limits of our measuring capabilities; sample permeabilities ranged from less than $1x10^{-9}$ to $3x10^{-3}$ Darcy (1 Darcy = 10^{-12} m^2). The lower limit for our measuring system was ±0.3 nDa. Absolute permeability uncertainties reported here are less than ±25% while relative uncertainties in a single experiment are 5 to 10%.

RESULTS

Permeability is plotted as a function of axial stress for a representative set of samples from the NIED borehole in Fig. 2. The first three measurements of each test at 10, 30, and 50 MPa were conducted without diviatoric stress and represent the permeability loss due to an increase in effective confining pressure. Permeability typically dropped by two orders of magnitude as microcracks closed in response to this hydrostatic loading. The remainder of the curves at axial stress above 50 MPa in Fig. 2 represent the deformation test at 50 MPa effective confining pressure. Initially, all samples showed loss of permeability with increasing diviatoric stress. By approximately 50% peak stress, most samples began to show increasing permeability with increasing diviatoric stress. This reversal from permeability decrease to permeability increase corresponds with the onset of dilatancy and the opening of microcracks within the sample (see, for example, [*Zoback and Byerlee*, 1975] and similar trends in electrical conductivity [*Lockner and Byerlee*, 1986]). The clay-rich shear zone core sample did not show dilatant behavior. Instead, it showed a steady loss of permeability with continued shearing and strain hardening. The protolith granodiorite shown in the bottom curve, Fig. 2, is a dense crystalline rock with low matrix permeability. Application of diviatoric stress reduced the permeability below the measurement threshold of our test system. By 400 MPa axial load, however, new dilatant cracks had increased permeability to a measurable level which continued to increase to peak axial load of 483 MPa. Another trend observable in Fig. 2 is a systematic decrease in peak strength of samples from the intact protolith, through the damage zone samples to the shear zone core sample. The low strength of the shear zone core is consistent with the concentration of shear deformation in this zone.

Rock Strength

Care was take during sample preparation to preserve the intrinsic grain structure and cohesion as much as possible. Obvious changes did occur in the samples due to drying and decompression of the original cores. However, these changes

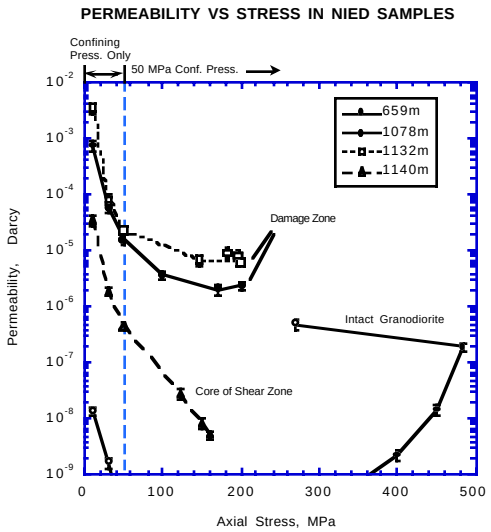

Figure 2. Permeability plotted versus axial load for selected NIED samples. Pressurization to 50 MPa is hydrostatic loading without diviatoric stress. Data above 50 MPa show permeability change in response to sample deformation at 50 MPa effective confining pressure.

were minimized as much as possible with the expectation that the *in situ* rock properties would be preserved to large extent. One way to evaluate this is to look for trends in the peak strength data for the various samples. Samples were tested at 50 MPa effective confining pressure, which is equivalent to approximately 3 km burial depth (assuming hydrostatic pore pressure gradient and average rock density of 2.7 g/cm^3), to provide an easy means of comparing sample to sample strength. Peak strength data are presented in Fig. 3 as the ratio of shear to normal stress (μ) resolved on a plane inclined 30° to the sample axis. The actual inclination of the fracture plane was difficult to determine in many of the strength tests, so that 30° provides a satisfactory approximation for comparison of different samples. Peak differential stress, σ_Δ, which is the quantity measured directly in the experiments, can be recovered from the data in Fig. 3 by the formula $\sigma_\Delta = 200\mu/(1.732-\mu)$ (in MPa). Normalized strength for the intact granodiorite protolith is μ_{intact}=1.18.

The horizontal axis in Fig. 3 is the horizontal distance between the shear zone axis and the *in situ* location of each core sample. No distinct shear zone axis could be identified for the deep NIED shear zone so the horizontal axis in Fig. 3d could be shifted by a few meters. Notice that the three fault crossings with well-defined shear zone cores (Figs. 3a, 3b and 3c) all show a minimum in strength at the shear zone axis. This is consistent with the model described above in which nearly all displacement occurs in the narrow fault core (a zone that is only a few centimeters wide in all three examples). The general trend in these three examples is for strength to gradually increase with distance away from the shear zone axis. This gradual strength increase corresponds to a decrease in microcrack damage (*i.e.*, Moore this volume and [*Moore and Lockner*, 1995]). Damage zone half-width as suggested by the strength data in Figs. 3a - 3c is 15 to 25 m.

The deep NIED shear zone (Fig. 4d) is different from the other three examples. No distinct shear zone core was observed in the borehole samples. While three of the core samples showed strength significantly less than the protolith strength ($\mu \sim 0.8$ as compared to 1.18), rock strength from this zone is significantly greater than the shallow shear zone core samples ($\mu \sim 0.6$). Apparently this deep zone was not activated in the Kobe earthquake and has, over time, been restrengthening by vein filling and mineral alteration.

Rock Matrix Permeability

We have already noted that the permeability of all samples tested shows a strong sensitivity to increases in effective confining pressure. The examples plotted in Fig. 2 all show a decrease of

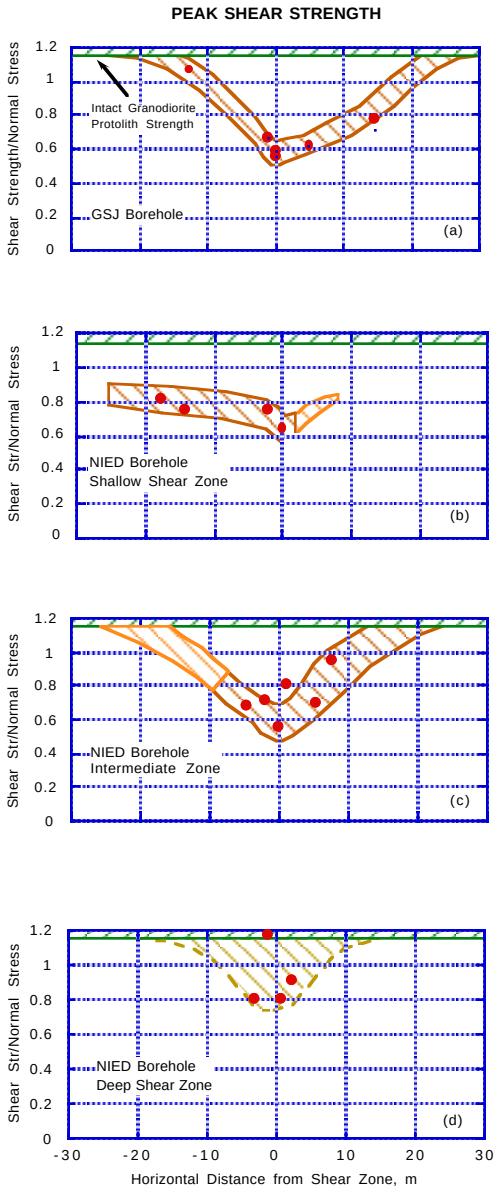

Figure 3. Profiles of peak shear strength divided by normal stress for the four shear zone crossings in the GSJ and NIED boreholes. Strength is lowest in the shear zone axis and recovers to the intact rock strength outside of the damage zone.

two orders of magnitude for a 50 MPa pressure increase. This pressure sensitivity is indicative of rocks in which flow is through low aspect ratio cracks (long, thin microcracks) which can open or close flow paths in response to small pressure changes. This type of microcrack is more susceptible to changes in permeability resulting from vein filling than the more equant pores that might be found, for example, in a porous sandstone.

Because of the strong pressure sensitivity of permeability in these samples, we expect that *in situ* permeability in the Nojima fault zone will decrease rapidly with depth. For example, the GSJ samples, with a fault crossing depth of 624 m would have an effective overburden pressure of approximately 11 MPa while the intermediate NIED crossing overburden pressure would be about 22 MPa. The peak damage zone permeabilities adjusted for these effective pressures would then be 3.3 mDa and 0.45 mDa, respectively.

To provide a more direct comparison of the different fault zone permeability measurements, we have plotted permeability profiles in Fig. 4 using values from 50 MPa effective confining pressure or 3 km burial depth. *In situ* permeabilities for the GSJ hole (at 11 MPa) would be about 50 times larger that the values shown in Fig. 4. As with the strength data, the three shallow crossings show permeability profiles similar to the idealized fault zone model described above. The shear zone axis, due to its high clay content and fine gouge grain size, has relatively low permeability in the microdarcy range. Flanking the shear zone axis, the highly fractured damage zone has permeabilities in the 50 to 100 microdarcy range. Farther away from the fault zone axis, grain damage and permeability decrease until permeability returns to the protolith permeability value. The damage zone half-width, as indicated by the permeability profiles ranges from 10 to 25 m. Based on trapped seismic wave analysis, Li *et al.* [1998] suggested a fault zone half width of approximately 15 m for the Nojima fault. Thus, direct measurements of both the permeability and strength of the fault zone indicate a damage zone half width that is consistent with the deeper seismic observations. The NIED borehole deep shear zone has permeability that is greater than the protolith permeability but significantly less

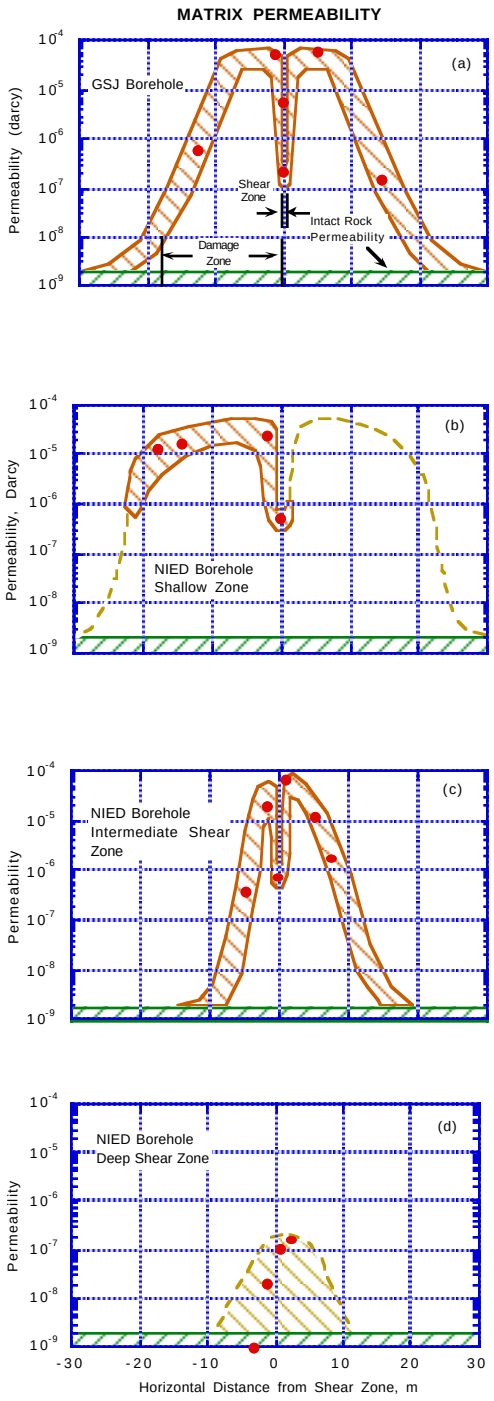

Figure 4. Profiles of matrix permeability measured at 50 MPa effective confining pressure. The three upper fault crossings show a low permeability shear zone axis surrounded by high permeability damage zones. The deep shear zone is partially sealed and was apparently not activated by the Kobe earthquake.

than the shallower shear zone values. Thus both strength and permeability data suggest that the deep shear zone was not activated in the Kobe earthquake and is now in the process of sealing and restrengthening.

DISCUSSION

Our measurements of core sample strength and permeability are in good agreement with the idealized fault zone model described, for example, by [*Chester et al.*, 1993; *Caine et al.*, 1996; *Evans et al.*, 1997]. We observe a thin, low-strength, low-permeability fault zone core flanked by zones of high permeability rock that have undergone relatively limited total shear. These observations imply that to depths of as much as 3 to 5 km, the post-seismic fault zone will act as a high permeability fluid conduit for fluid flow in the plane of the fault. Because the fault core has low permeability it is likely to act as a barrier to fluid flow across the fault. However, this barrier is notably thin and may have a complex structure. For example, the Nojima fault zone appears to have branched into two shear zones between the GSJ and NIED borehole crossings. To the degree that this thin shear zone core is spatially discontinuous and anastomosed, its ability to act as a fluid barrier will be diminished.

The observations reported here provide a unique opportunity to understand fault zone properties at depth following a damaging earthquake. While we do not know the mechanical and hydraulic properties of the Nojima fault before the Kobe earthquake, it is likely that the violent rupture of the fault led to a sudden increase in permeability. This is consistent with observations following the 1989 Loma Prieta earthquake that enhanced fluid flow occurred in the epicentral region [*Rojstaczer and Wolf*, 1992]. One important question not addressed by this study is how rapidly the enhanced fault zone permeability structure will be reduced by sealing and crack healing processes. The observation of increased strength and decreased permeability in the deep NIED shear zone indicate that these processes can have significant influence on fault zone mechanics over the lifetime of an active fault. If this sealing and restrengthening process can occur over a single earthquake cycle, it could have an important influence on repeat time, stress drop and rupture nucleation.

REFERENCES

Ben-Zion, Y., Properties of seismic fault zone waves and their utility for imaging low-velocity structures, *J. Geophys. Res., 103*, 12,567-12,585, 1998.

Caine, J. S., J. P. Evans, and C. B. Forster, Fault zone architecture and permeability structure, *Geology, 24*, 1025-1028, 1996.

Caine, J. S., and C. B. Forster, Fault zone architecture and fluid flow: Insights from field data and numerical modeling, in *Faults and Subsurface Flow in the Shallow Crust: AGU Geophysical Monograph, Vol. 113*, edited by Haneberg, Amer. Geophys. Union, Washington, D.C., 1999.

Chester, F. M., J. P. Evans, and R. L. Biegel, Internal structure and weakening mechanisms of the San Andreas fault, *J. Geophys. Res., 98*, 771-786, 1993.

Evans, J. P., C. B. Forster, and J. V. Goddard, Permeability of fault-related rocks, and implications for hydraulic structure of fault zones, *J. Structural Geol., 19*, 1393-1404, 1997.

Li, Y.-G., K. Aki, J. E. Vidale, and M. G. Alvarez, A delineation of the Nojima fault ruptured in the M7.2 Kobe, Japan, earthquake of 1995 using fault zone trapped waves, *J. Geophys. Res., 103*, 7247-7263, 1998.

Li, Y.-G., and P. Leary, Fault zone seismic trapped waves, *Bull. Seismol. Soc. Am., 80*, 1245-1271, 1990.

Lockner, D. A., and J. D. Byerlee, Changes in complex resistivity during creep in granite, *Pure and Appl. Geophys., 124*, 659-676, 1986.

Moore, D. E., and D. A. Lockner, The role of microcracking in shear-fracture propagation in granite, *J. Struct. Geol., 17*, 95-114, 1995.

Rojstaczer, S., and S. Wolf, Permeability changes associated with large earthquakes: An example from Loma Prieta, California, *Geology*, 211-214, 1992.

Zoback, M. D., and J. D. Byerlee, The effect of microcrack dilatancy on the permeability of Westerly granite, *J. Geophys. Res., 80*, 752-755, 1975.

(in Proc. of the Internat. Wrkshp on the Nojima Fault Core and Borehole Data Analysis, Tsukuba, Japan, Nov 22-23, 1999, USGS Open File Report 00-129, H. Ito, K. Fujimoto, H. Tanaka, and D. Lockner, editors, pp. 147-152)